

**This item is the archived peer-reviewed author-version of:**

Engineering aspects for the design of a bicarbonate zero-gap flow electrolyzer for the conversion of CO<sub>2</sub> to formate

**Reference:**

Gutiérrez Sánchez Oriol, De Mot Bert, Bulut Metin, Pant Deepak, Breugelmans Tom.- Engineering aspects for the design of a bicarbonate zero-gap flow electrolyzer for the conversion of CO<sub>2</sub> to formate  
ACS applied materials and interfaces - ISSN 1944-8252 - 14:27(2022), p. 30760-30771  
Full text (Publisher's DOI): <https://doi.org/10.1021/ACSAMI.2C05457>  
To cite this reference: <https://hdl.handle.net/10067/1893330151162165141>

# 1 **Engineering Aspects for the Design of a Bicarbonate Zero-Gap Flow** 2 **Electrolyzer for the Conversion of CO<sub>2</sub> to Formate**

3  
4 Oriol Gutiérrez-Sánchez<sup>a,b,1</sup>, Bert de Mot<sup>a,1</sup>, Metin Bulut<sup>b</sup>, Deepak Pant<sup>b,c</sup> and Tom  
5 Breugelmans<sup>\*a,c</sup>

6  
7 <sup>a</sup> University of Antwerp, Research Group Applied Electrochemistry and Catalysis  
8 (ELCAT), Universiteitsplein 1, 2610 Wilrijk, Belgium.

9 <sup>b</sup> Separation and Conversion Technology, Flemish Institute for Technological Research  
10 (VITO), Boeretang 200, Mol 2400, Belgium.

11 <sup>c</sup> Centre for Advanced Process Technology for Urban Resource Recovery (CAPTURE),  
12 Frieda Saeystraat 1, 9052 Zwijnaarde, Belgium

13 \* Corresponding author: [tom.breugelmans@uantwerpen.be](mailto:tom.breugelmans@uantwerpen.be)

14  
15 <sup>1</sup> These authors contributed equally.

## 16 **Abstract**

17  
18 CO<sub>2</sub> electrolyzers require gaseous CO<sub>2</sub> or saturated CO<sub>2</sub> solutions to achieve high energy  
19 efficiency (EE) in flow reactors. However, CO<sub>2</sub> capture and delivery to electrolyzers is in most  
20 cases responsible for the inefficiency of the technology. Recently, bicarbonate zero-gap flow  
21 electrolyzers have proven to convert CO<sub>2</sub> directly from bicarbonate solutions, thus mimicking  
22 a CO<sub>2</sub> capture media, obtaining high Faradaic efficiency (FE) and partial current density (CD)  
23 towards carbon products. However, since bicarbonate electrolyzers use bipolar membrane  
24 (BPM) as a separator, the cell voltage ( $V_{\text{Cell}}$ ) is high and the system becomes less efficient  
25 compared to analogous CO<sub>2</sub> electrolyzers. Due to the role of the bicarbonate both as a carbon  
26 donor and proton donor (in contrast with gas-fed CO<sub>2</sub> electrolyzers), optimization by using  
27 know-how from conventional gas-fed CO<sub>2</sub> electrolyzers is not valid. In this study, we have  
28 investigated how different engineering aspects, widely studied for upscaling gas-fed CO<sub>2</sub>  
29 electrolyzers, influence the performance of bicarbonate zero-gap flow electrolyzers when  
30 converting CO<sub>2</sub> to formate. The temperature, the flow rate and the concentration of electrolyte  
31 are evaluated in terms of FE, productivity,  $V_{\text{Cell}}$  and EE in a broad range of current densities (10-

32 400 mA cm<sup>-2</sup>). CD of 50 mA cm<sup>-2</sup>, room temperature, high flow rate (5 mL cm<sup>-2</sup>) of electrolyte  
33 and high carbon load (KHCO<sub>3</sub> 3 M) are proposed as potentially optimal parameters to  
34 benchmark a design to achieve the highest EE (27% is obtained this way), one of the most  
35 important criteria when upscaling and evaluating Carbon Capture & Conversion technologies.  
36 On the other hand, at high CD (>300 mA cm<sup>-2</sup>), low flow rate (0.5 mL cm<sup>-2</sup>) has the highest  
37 interest for downstream processing (>40 g L<sup>-1</sup> formate is obtained this way) at the cost of a low  
38 EE (<10 %).

### 39 **Keywords**

40 Carbon Capture and Utilization, bicarbonate reduction, electrochemical CO<sub>2</sub> reduction, zero-  
41 gap flow electrolyzer, bipolar membrane

### 42 **1 Introduction**

43 The increase in the concentration of CO<sub>2</sub> present in the atmosphere, currently over 415 ppm,  
44 poses a threat to society since it is directly linked to global warming and climate change.<sup>1</sup> The  
45 CO<sub>2</sub> is mostly released from anthropogenic sources as a co-product of many processes within  
46 the chemical industry (like organic synthesis or metallurgy) or after the combustion of fuels  
47 as a means of energy obtention.<sup>2,3</sup> Some of the strategies to reduce the net emissions is to  
48 reutilize the released CO<sub>2</sub> by developing technologies in the theme of Carbon Capture and  
49 Utilization (CCU). In CCU, the CO<sub>2</sub> is directly captured from the air (DAC) or from flue gasses  
50 to be used as a substrate to produce high-value or bulk chemicals with processes such as  
51 methanation or electroreduction.<sup>4,5</sup> The electrocatalytic conversion of CO<sub>2</sub> (eCO<sub>2</sub>R) is  
52 proposed as one of the most promising technologies to convert CO<sub>2</sub> in an efficient and green  
53 way after it has been captured.<sup>6</sup> The eCO<sub>2</sub>R converts CO<sub>2</sub> to a variety of carbon-based products  
54 (such as formate, CO, ethylene, methane and alcohols) by using renewable electricity and an  
55 electrocatalyst, which will determine the product formed.<sup>7-10</sup> However, one of the main  
56 drawbacks is the high energy requirement for capturing CO<sub>2</sub>, specifically from the air.<sup>11,12</sup> Since  
57 the concentration of CO<sub>2</sub> in the air is relatively very low, obtaining it becomes cumbersome  
58 and costly. Current technologies to capture CO<sub>2</sub> include a capturing step with an alkaline  
59 solution, a regeneration step to extract back the CO<sub>2</sub> and a compression step to store the CO<sub>2</sub>  
60 to be delivered later to the electrochemical cell.<sup>13-15</sup> The last two steps require most of the

61 total energy for capturing and converting CO<sub>2</sub>. Then, capturing and delivering the CO<sub>2</sub>  
62 efficiently to the electrochemical cell is critical to making the process feasible and industrially  
63 interesting.

64 To avoid these high energy demanding steps, one of the alternatives is to use bicarbonate  
65 (HCO<sub>3</sub><sup>-</sup>) aqueous solutions, such as KHCO<sub>3</sub>, as the actual reactant for the electrochemical  
66 reduction step instead of gaseous CO<sub>2</sub> or CO<sub>2</sub> purged solutions.<sup>16</sup> By using bicarbonate as  
67 substrate, there is no necessity of compressing and releasing CO<sub>2</sub> again after the capturing  
68 step, since CO<sub>2</sub> is captured in form of bicarbonate with an alkaline solution, like KOH, and then  
69 used directly. Although this alternative appears to solve the drawback of using CO<sub>2</sub> gas as a  
70 substrate, it is still far from applicable. Bicarbonate electrolysis has proven to be less efficient  
71 in terms of Faradaic Efficiency (FE) and partial current density (CD) towards carbon products  
72 compared to analogous gas-fed CO<sub>2</sub> reduction systems and little research has been done  
73 about it. Most of the studies currently done on eCO<sub>2</sub>R involve supplying pure CO<sub>2</sub> gas to the  
74 electrochemical cell or gas diffusion electrodes instead of using post-capture CO<sub>2</sub> solutions,<sup>17</sup>  
75 mostly due to the little knowledge that the community possessed on the role of bicarbonate  
76 as a substrate (or intermediate) in eCO<sub>2</sub>R.

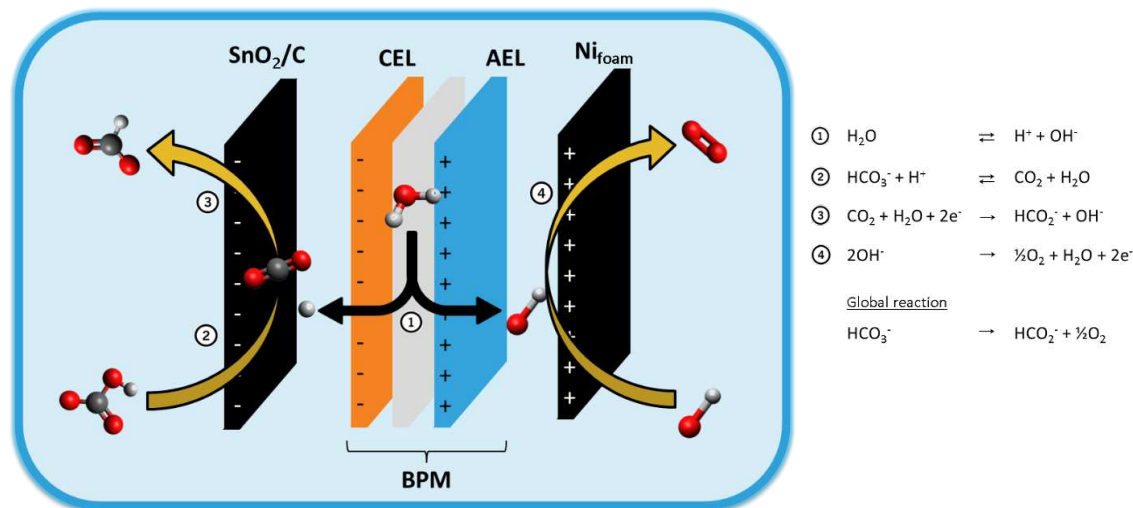
77 The role of bicarbonate in the eCO<sub>2</sub>R and the mechanism behind the electrochemical  
78 reduction of bicarbonate have been debated within the community for a long time. It is said  
79 that bicarbonate is the substrate of the reduction reaction and thus the low FE comes from  
80 the lack of the right catalyst or the unoptimized electrochemical reactor,<sup>18,19</sup> while on the  
81 other hand there is also the statement supporting that bicarbonate is merely a carbon donor,  
82 CO<sub>2</sub> being the substrate of the reaction (delivered from the equilibrium reaction of  
83 bicarbonate with water) and that the low FE comes from the high proton donor ability of  
84 bicarbonate, thus promoting the hydrogen evolution reaction (HER), the main co-reaction.<sup>20</sup>  
85 Based on the research done on this topic in the last few years, it can be concluded that in fact  
86 1) bicarbonate is a carbon donor and supplies CO<sub>2</sub> to the electrode;<sup>21,22</sup> 2) bicarbonate is an  
87 even better proton donor, promoting the HER;<sup>20,23</sup> and 3) the substrate is indeed CO<sub>2</sub> instead  
88 of bicarbonate, even in pure bicarbonate solutions.<sup>24</sup> Then, to increase the FE and CD towards  
89 carbon products when using bicarbonate as a substrate there are two main strategies to  
90 follow: either the proton donor ability of bicarbonate is inhibited or the carbon donor ability  
91 of bicarbonate is promoted.

92 Some studies explored how to inhibit HER in bicarbonate electroreduction systems but,  
93 although high FE was obtained (more than 70%), the partial CD was low ( $3 \text{ mA cm}^{-2}$ ) and the  
94 strategy approached involved the addition of extra components to the electrolyte, such as  
95 surfactants, that made the system more complex and harder to upscale.<sup>24,25</sup> On the other  
96 hand, some other studies explored how to improve the carbon donor ability of bicarbonate  
97 by acidifying in situ the catholyte (and thus releasing more  $\text{CO}_2$  from bicarbonate) by using a  
98 bipolar membrane (BPM) as a separator in a zero-gap flow electrolyzer, depleting water to  $\text{H}^+$   
99 (towards the catholyte) and  $\text{OH}^-$  (towards the anolyte) upon the polarization of the electrodes  
100 (Figure 1). The results obtained by using this strategy were promising, specifically in terms of  
101 partial CD ( $50\text{-}150 \text{ mA cm}^{-2}$ ), and good FE towards formate or CO was obtained (40-60%).<sup>26,27</sup>  
102 However, since a BPM has a three-membrane layer configuration, the ohmic drop between  
103 the two electrodes is very high. In addition, an overpotential for water dissociation is added  
104 to the system thus becoming more inefficient in terms of energy efficiency of the  
105 electrochemical cell (EE) than in analogous systems involving  $\text{CO}_2$  gas and ionomeric  
106 membranes (because of the increase in the cell voltage,  $V_{\text{Cell}}$ ).<sup>28-30</sup> Nevertheless, due to its  
107 special role in bicarbonate electrolysis, the use of BPM is benchmarked for the design of  
108 bicarbonate (zero gap) electrolyzers.

109 As the most promising strategy, there is interest in optimizing the performance of the  
110 bicarbonate zero-gap electrolyzer involving BPM as a separator. The first approach was to find  
111 the most optimal configuration of the electrocatalyst to achieve the highest FE and partial CD  
112 towards carbon products. Most  $\text{eCO}_2\text{R}$  flow electrolyzers involve Gas Diffusion Electrodes  
113 (GDE) to avoid flooding of the electrode while the  $\text{CO}_2$  is provided from the gas phase.<sup>17</sup> To  
114 achieve these functions, the GDEs are generally formed of carbon support, a Micro-Porous  
115 Layer (MPL) and a hydrophobic PTFE layer. Since in bicarbonate electrolyzers the  $\text{CO}_2$  is  
116 delivered from the bicarbonate electrolyte, this electrocatalyst configuration was suboptimal.  
117 Lees *et al.* investigated the effect of the different layers present in a GDE for bicarbonate  
118 electrolysis. They proposed an optimal configuration of the electrocatalyst where the MPL  
119 and PTFE layers are removed from the GDE. The increase in the hydrophobicity of the  
120 electrode was detrimental for the diffusion of  $\text{CO}_2$  from bicarbonate (partial flooding of the  
121 electrode is of interest in bicarbonate electrolyzers), thus decreasing the FE and partial CD.<sup>31</sup>

122 Other than investigating the configuration of the electrode, there is a lack of detailed research  
123 on other engineering aspects for bicarbonate electrolysis. Therefore, there is still room for  
124 improvement on the optimization of a bicarbonate zero-gap flow electrolyzer. For this reason,  
125 we have investigated how operational parameters such as the temperature of the reactor,  
126 the inlet flow rate of the electrolyte and the concentration of carbon load affect the  
127 performance of a bicarbonate zero-gap flow electrolyzer involving a BPM. In addition, we  
128 have complemented the study on the optimization of the electrocatalyst done by Lees *et al.*,  
129 by investigating the effect of the binder material used in the composition of the  
130 electrocatalyst ink on the performance of the system. Formate is targeted as product for the  
131 electrolysis experiments. It is well known that formic acid is one of the key products for the  
132 valorization of eCO<sub>2</sub>R.<sup>32</sup> However, currently, eCO<sub>2</sub>R strategies pursues formate, too.<sup>33</sup> This is  
133 due to the low pK<sub>a</sub> of formic acid (3.74) which requires an acidic catholyte (thus promoting  
134 HER) or high concentration of formic acid at the outlet catholyte, otherwise formate is  
135 produced. This is hardly possible in bicarbonate electrolysis because of the mild-alkaline  
136 media of the catholyte (pH 8-9) and the buffering effect of bicarbonate. State-of-the-art in  
137 eCO<sub>2</sub>R already considers formate as value product for energy storage, such as in formate fuel  
138 cells.<sup>34,35</sup> On the other hand, some downstream processing pathways already includes the  
139 conversion of formate to formic acid prior the separation steps. In some cases, even formate  
140 is directly separated without the necessity of converting it to formic acid first.<sup>33</sup> Therefore,  
141 formate is an ideal product to test the operational conditions of bicarbonate electrolysis.  
142 Therefore, Sn-based electrocatalyst was selected to convert bicarbonate since it is one of the  
143 most selective materials for the production of formate in eCO<sub>2</sub>R.<sup>36</sup> In addition, Sn has never  
144 been tested before in bicarbonate electrolysis, adding extra value to the study (only Bi has  
145 been reported).<sup>37</sup> Nevertheless, the FE towards formate from bicarbonate electrolysis is still  
146 far from optimal (up to 60% has been reported up to day),<sup>26</sup> then we must assume an  
147 important fraction of the FE towards co-reactions such as the HER and the CO formation.  
148 Based on our previous work on CO<sub>2</sub> electrolysis (where similar catalyst configuration and  
149 operational conditions were used)<sup>38</sup> and the reports on alkaline CO<sub>2</sub>/bicarbonate  
150 electrolysis,<sup>36</sup> the main products are formate and H<sub>2</sub>. Therefore, we find negligible for this  
151 study the fraction of CO formed from bicarbonate electrolysis, thus considering the rest of  
152 the FE towards HER. Nonetheless, in research focused on CO/syngas production or in studies  
153 on the selectivity of bicarbonate electrolysis, this small fraction of FE (specifically how it

154 evolves with high CD) must be considered. Nevertheless, the conclusions of the results  
 155 obtained in this study can be easily extrapolated to other targeted products, such as CO, since  
 156 the same reactor configuration is currently used.



157  
 158 **Figure 1: Schematic representation of the mechanism of bicarbonate electrochemical**  
 159 **reduction to formate in reactors involving a BPM (CEL: Cation Exchange Membrane. AEL:**  
 160 **Anion Exchange Membrane).**

161 The FE towards formate ( $\text{FE}_{\text{Formate}}$ ), formate concentration,  $V_{\text{Cell}}$  and EE were used to evaluate  
 162 and compare the performance of the electrolyzer in each case scenario for a broad range of  
 163 current densities ( $10\text{-}400 \text{ mA cm}^{-2}$ ). The details, assumptions and formulas used can be found  
 164 in the supporting information. The FE allowed us to evaluate the selectivity of the electrolysis,  
 165 the formate concentration allowed us to evaluate the profitability of the product solution for  
 166 downstream processing, the  $V_{\text{Cell}}$  allowed us to evaluate the cell efficiency (CE) of the  
 167 electrolyzer and finally, the EE allowed us to evaluate the overall efficiency of the electrolysis  
 168 (for upscaling prospects). For the evaluation of the effect of the binder material in the  
 169 configuration of the electrode, only the FE was evaluated. At the end of this study, the most  
 170 optimal configuration(s) are proposed for benchmarking high-efficient engineering aspects  
 171 for the design of a bicarbonate zero-gap flow electrolyzer.

172  
 173

## 174 2 Materials and methods

### 175 2.1 Materials and solutions

176 All the chemicals were obtained from commercial sources and used without purification unless  
177 stated otherwise.  $\text{KHCO}_3$  solutions used as catholyte were prepared by dissolving the  
178 corresponding amount of 3 M (unless stated otherwise) potassium hydrogen carbonate 99.5%  
179 (Chem-Lab) in Ultra-Pure water (MilliQ, 18.2  $\text{M}\Omega$  cm). The KOH solutions used as anolyte were  
180 prepared by dissolving the corresponding amount of 1 M of potassium hydroxide pellets  
181 (Chem-Lab) in Ultra-Pure water. Tin nanoparticles, particle size <150 nm (Sigma-Aldrich) and  
182 tin(IV) oxide nanoparticles (Sigma-Aldrich), particle size  $\leq 100$  nm were used as the catalyst and  
183 porous carbon paper AvCarb MGL 190 (Fuel Cell Store) was used as catalyst support. Nafion D-  
184 520 dispersion (Alfa Aesar) and Sustanion<sup>®</sup> XA-9 (Dioxide Materials) were used as binder  
185 ionomer during electrode manufacturing. For the counter electrode, Ni foam (Nanografi) was  
186 used. To separate the catholyte and the anolyte, a Bipolar Membrane (FumaSep) was used.

### 187 2.2 Working electrode manufacturing

188 Adding complexity to the electrocatalyst material has been questioned due to the unrealistic  
189 upscaling capabilities, even though the electrochemical response in lab-scale is proficient. For  
190 instance, complex electrodes that consists of multiple components such as nano-scaled  
191 arrangements, binders or additives present a huge variety of properties (conductivity, active  
192 sites, stability...) that, as a result, make the chemistry/structure of the surface almost  
193 impossible to correlate.<sup>39</sup> To benchmark our experimental procedure and to focus specifically  
194 on the engineering parameters of the reactor mentioned, commercial Sn (or  $\text{SnO}_2$ )  
195 nanoparticles of particle size <150 nm are used. Del Castillo *et al.* demonstrated an optimal  
196 reduction of  $\text{CO}_2$  to formate on by using these Sn particles with a particle size of 150 nm.<sup>40</sup> We  
197 used this procedure in previous  $\text{eCO}_2\text{R}$  engineering studies and it allowed a proper evaluation  
198 of the results obtained as well as good reproducibility.<sup>41</sup> Parallely, we used  $\text{SnO}_2$  particles,  
199 too, as high performance has been observed in recent studies.<sup>42,43</sup>

200 Working electrodes were manufactured by spray coating a catalyst ink on top of a  $4 \times 4$   $\text{cm}^2$   
201 porous carbon paper. For the preparation of this ink, the nanoparticles (Sn or  $\text{SnO}_2$ ) were mixed  
202 with a 50/50 isopropanol/water solution. Optionally a binder ionomer was added to the  
203 mixture following the procedure benchmarked in our previous research (mass ratio of 70/30



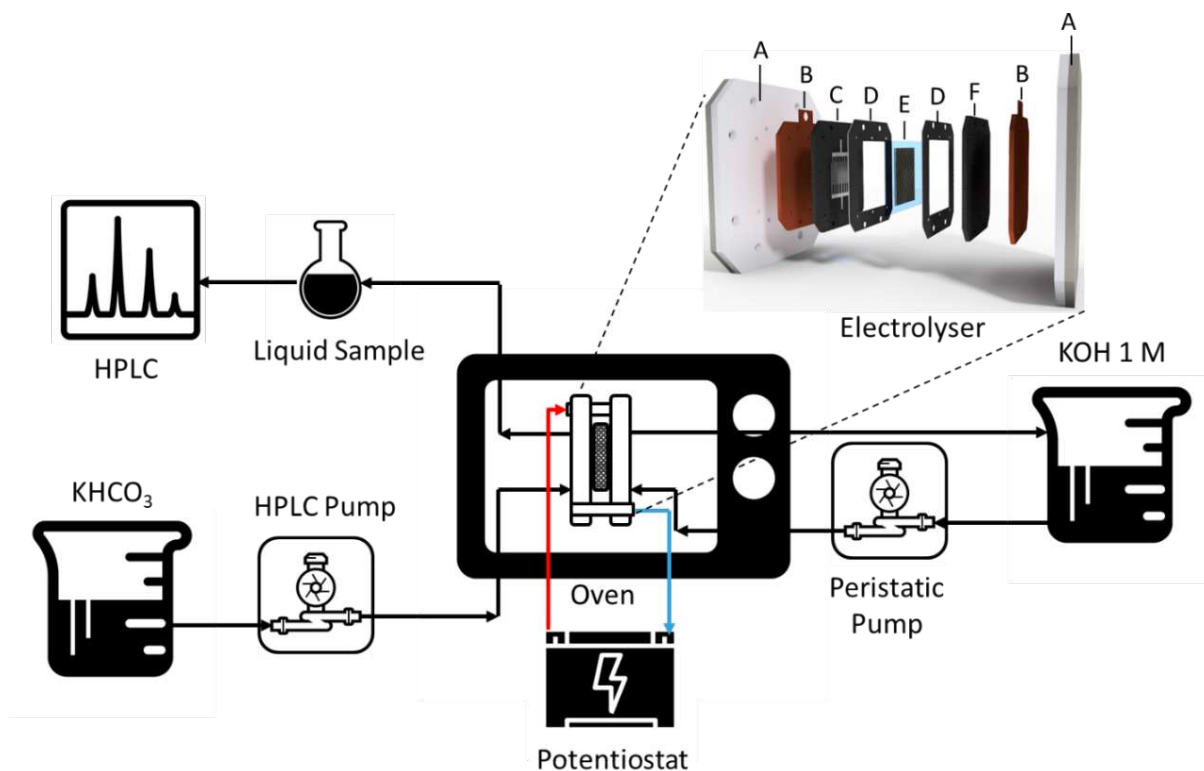
204 nanoparticles/binder and concentration of 3 wt%).<sup>38</sup> Next a sonication probe (SinapTec  
205 NexTgen Lab 120) was used for 30 minutes to disperse the nanoparticles in the solution and  
206 create a homogenous ink. After the sonication procedure, the homogenous ink is deposited on  
207 the porous carbon substrate by airbrushing with argon as carrier gas. During the airbrushing  
208 procedure, the electrode was placed on a hotplate where the temperature was maintained at  
209 60 °C to promote the evaporation of the solvent. Finally, the finished electrode is dried under  
210 atmospheric conditions and weighed to calculate the loading of the catalyst particles. All  
211 electrodes used in the experiments had a final loading of  $2.0 \pm 0.2 \text{ mg cm}^{-2}$  nanoparticles.

### 212 *2.3 Electrolysis*

213 The electrochemical screening is performed in a custom build bicarbonate electrolyzer, of  
214 which a schematic presentation is shown in Figure 2. The electrolyte was not previously purged  
215 with an inert gas to mimic as better as possible a CO<sub>2</sub> capture solution. Then, O<sub>2</sub> reduction and  
216 CO production are assumed as artefacts of the process and as contributors to the total FE. The  
217 bicarbonate enters the electrolyzer from the bottom, where it flows through the graphite flow  
218 channel to the top of the electrolyzer. The graphite flow channel has an interdigitated design,  
219 thereby the bicarbonate is convectively forced in the pores of the working electrode which is  
220 pressed against the graphite plate. This flow design thereby optimizes the mass transfer of  
221 bicarbonate towards the catalyst surface. On top of the electrode, a BPM is placed. This BPM  
222 serves multiple purposes. 1) It separates the cathode from the anode region and thereby  
223 prevents product crossover; 2) allows the movement of ions in between the two electrodes  
224 and 3) provides the protons to the catholyte. The last purpose is essential for the good  
225 operation of the cell as the protons will dissociate the bicarbonate in water and CO<sub>2</sub>. The anode  
226 side of the electrolyzer is similar to the previously described cathode side. However, here a  
227 nickel foam was used as an electrode and potassium hydroxide as an anolyte. Copper current  
228 collectors are fitted against the backs of the graphite flow channels and are used to connect  
229 the potentiostat (Autolab PGSTAT302N) to the system. Finally, the electrolyzer is assembled  
230 using two aluminium backplates and Viton gaskets to provide sealing.

231 The bicarbonate solution was fed in single-pass mode to the cathode side of the electrolyzer  
232 using a High-Performance Liquid Chromatography (HPLC) pump which allowed for accurate  
233 control of the flowrate. At the outlet of the electrolyzer, a liquid/gas separator was used to

234 separate the different phases of the flow exiting the reactor and samples were taken for  
235 product analysis. On the anode side, a peristaltic pump was used to recirculate 1000 mL of 1  
236 M potassium hydroxide at a flow rate of  $20 \text{ mL min}^{-1}$ . The complete electrolyzer was placed in  
237 an oven (Binder Oven) to control the temperature of the system at multiple values (25, 40 and  
238  $60 \text{ }^\circ\text{C}$ ).



239

240 **Figure 2: Schematic representation of the experimental set-up of the zero-gap electrolyzer for**  
241 **bicarbonate electrochemical reduction. Expanded view: A) end-plates; B) Cu current collectors;**  
242 **C) Cathode flow channel; D) Catalysts gaskets; E) BPM; F) Anode flow channel.**

#### 243 *2.4 Product analysis*

244 For product analysis, Agilent 1200 High-Performance Liquid Chromatography with Agilent Hi-  
245 Plex H 7.7×300 mm column was used to separate the product and Agilent 1260 RID detector  
246 to detect and quantify formate in the form of formic acid. The samples were previously diluted  
247 with water and acidified with H<sub>2</sub>SO<sub>4</sub> to avoid bubble formation and obstruction in the column.  
248 H<sub>2</sub>SO<sub>4</sub> 0.01 M was used as the mobile phase. Two tests per set of experiments are performed  
249 and displayed as the average of FE, the concentration of formate, Cell Voltage and EE. The  
250 error bars correspond to the standard deviation.

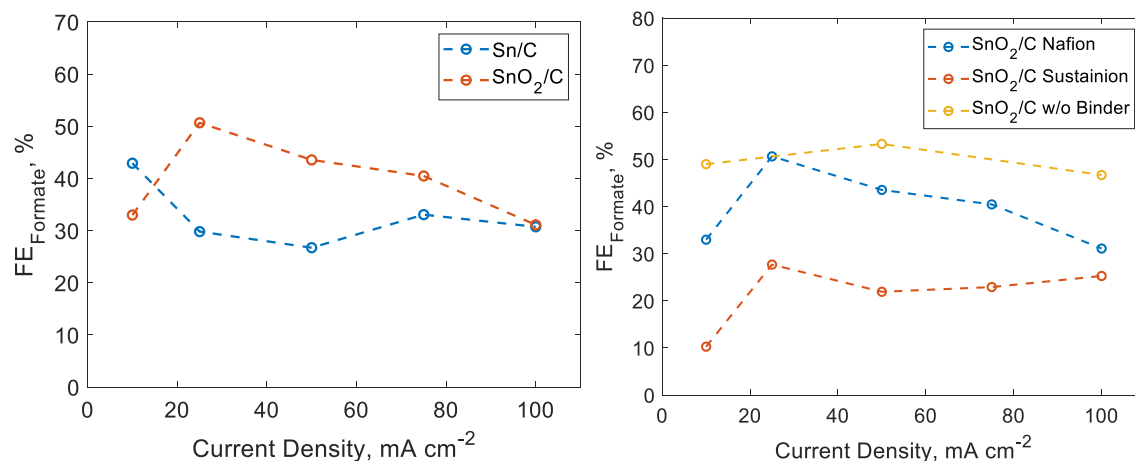
## 251 3 Results and Discussion

### 252 3.1 Catalyst configuration: binder material and oxidation state

253 Tin-based catalysts are already well established among the preferred catalyst for the eCO<sub>2</sub>R  
254 towards formate. Recently it was shown that oxidized (IV) tin performed even better.<sup>44–46</sup> To  
255 analyse if this behaviour remains in a bicarbonate electrolyzer, we have performed  
256 experiments with porous carbon on which either Sn or SnO<sub>2</sub> nanoparticles were deposited.  
257 The results displayed in Figure 3 (left) show that at low current densities (10 mA cm<sup>-2</sup>) the  
258 FE<sub>Formate</sub> is slightly better on Sn (38%) versus SnO<sub>2</sub> (33%). However, by increasing the CD a drop  
259 in FE<sub>Formate</sub> on Sn was observed, while on SnO<sub>2</sub> drastically increased. At 25 mA cm<sup>-2</sup>, the  
260 FE<sub>Formate</sub> on SnO<sub>2</sub> nanoparticles reached a peak at 51% after which it linearly decreased to 31%  
261 at 100 mA cm<sup>-2</sup>. On Sn nanoparticles, the FE<sub>Formate</sub> drops 29% at 25 mA cm<sup>-2</sup>. Further increase  
262 of the current had little effect as the FE<sub>Formate</sub> stabilized at 30%. From these results, it is clear  
263 that in analogy to eCO<sub>2</sub>R electrolyzers, SnO<sub>2</sub> outperforms Sn.

264 Since in bicarbonate electrolyzers there is high competition with HER, we also evaluated the  
265 effect of the binder material used in the manufacturing of the working electrodes. The binder  
266 may have an impact on the performance of the reactor, caused by the high proton activity at  
267 the catalyst surface due to the high rate of protons generated at the BPM surface, in  
268 combination with the binder effect. A proton exchange binder such as Nafion promotes the  
269 transfer of H<sup>+</sup> to the catalytic surface, promoting HER, while an anion exchange binder like  
270 Sustainion promotes the transfer of bicarbonate ions (also a good proton donor) promoting  
271 HER as well. Overall, these phenomena promote HER and thereby lower the FE and partial CD  
272 towards formate. However, there are studies showing up the good performance of Sustainion  
273 membranes in diffusing CO<sub>2</sub> and decrease HER.<sup>47</sup> Nevertheless, these studies are focused on  
274 gas-fed electrolyzers and do not include high concentrated bicarbonate solutions as  
275 catholyte, therefore the influence of the diffusion of bicarbonate anion is hardly comparable  
276 to our system. Nevertheless, it is interesting to observe if the good CO<sub>2</sub>-diffusion properties  
277 of Sustainion overcomes the diffusion of bicarbonate anion to the surface of the electrode  
278 and thus HER. The data shown in Figure 3 (right) further confirms that the performance of the  
279 bicarbonate electrolyzer was altered when different binder materials were used during the  
280 production process of the catalyst layer. Here the data is presented for porous carbon-coated  
281 with SnO<sub>2</sub> catalyst and either Nafion, Sustainion or no binder present. Both the Nafion and

282 Sustainion® binders show similar behaviour, the decrease of  $FE_{\text{Formate}}$ . At low CD the  $FE_{\text{Formate}}$   
 283 is low. Then increasing the CD leads to a peak  $FE_{\text{Formate}}$  at 25  $\text{mA cm}^{-2}$  (27% and 51% for  
 284 Sustainion and Nafion respectively) and a further increase of CD results in the stabilization of  
 285  $FE_{\text{Formate}}$ . Nevertheless, Nafion outperforms Sustainion since the concentration of bicarbonate  
 286 anions is substantially higher than protons. It is shown how the diffusion of bicarbonate anion  
 287 outperforms the diffusion of  $\text{CO}_2$  with Sustainion, resulting in a decrease of  $FE_{\text{Formate}}$  compared  
 288 to Nafion and no-binder instead to an increase. Again, the performance of the electrolyzer in  
 289 terms of  $FE_{\text{Formate}}$  was severely limited due to the favouring of HER. When no binder was used,  
 290 the  $FE_{\text{Formate}}$  remained constant around 50%, increasing slightly to 54% at 50  $\text{mA cm}^{-2}$ , in  
 291 contrast to the experiments with a binder, where a decrease in performance when the CD  
 292 increased occurred.



293  
 294 **Figure 3:  $FE_{\text{Formate}}$  when using Sn or SnO<sub>2</sub> nanoparticles as electrocatalysts on top of a porous**  
 295 **carbon substrate (left).  $FE_{\text{Formate}}$  when using a SnO<sub>2</sub>/C catalyst with a Nafion binder, a**  
 296 **Sustainion binder or without a binder (right). All the experiments were performed using a**  
 297 **KHCO<sub>3</sub> 3 M solution at 5  $\text{mL min}^{-1}$  and 25 °C.**

298 Based on these experimental results and due to this study is not focused on the stability of  
 299 the electrocatalyst, we decided to avoid using a binder as part of the ink for electrode  
 300 manufacturing. We understand that, by not incorporating the binder, the stability of the  
 301 electrode is compromised (as will be discussed further). However, obtaining higher FE (and  
 302 thus higher absolute values) facilitated the evaluation and comparison of the different  
 303 experimental results obtained in this study. It is worth mentioning that the results obtained  
 304 in this section adds further knowledge in the field of developing electrocatalyst for

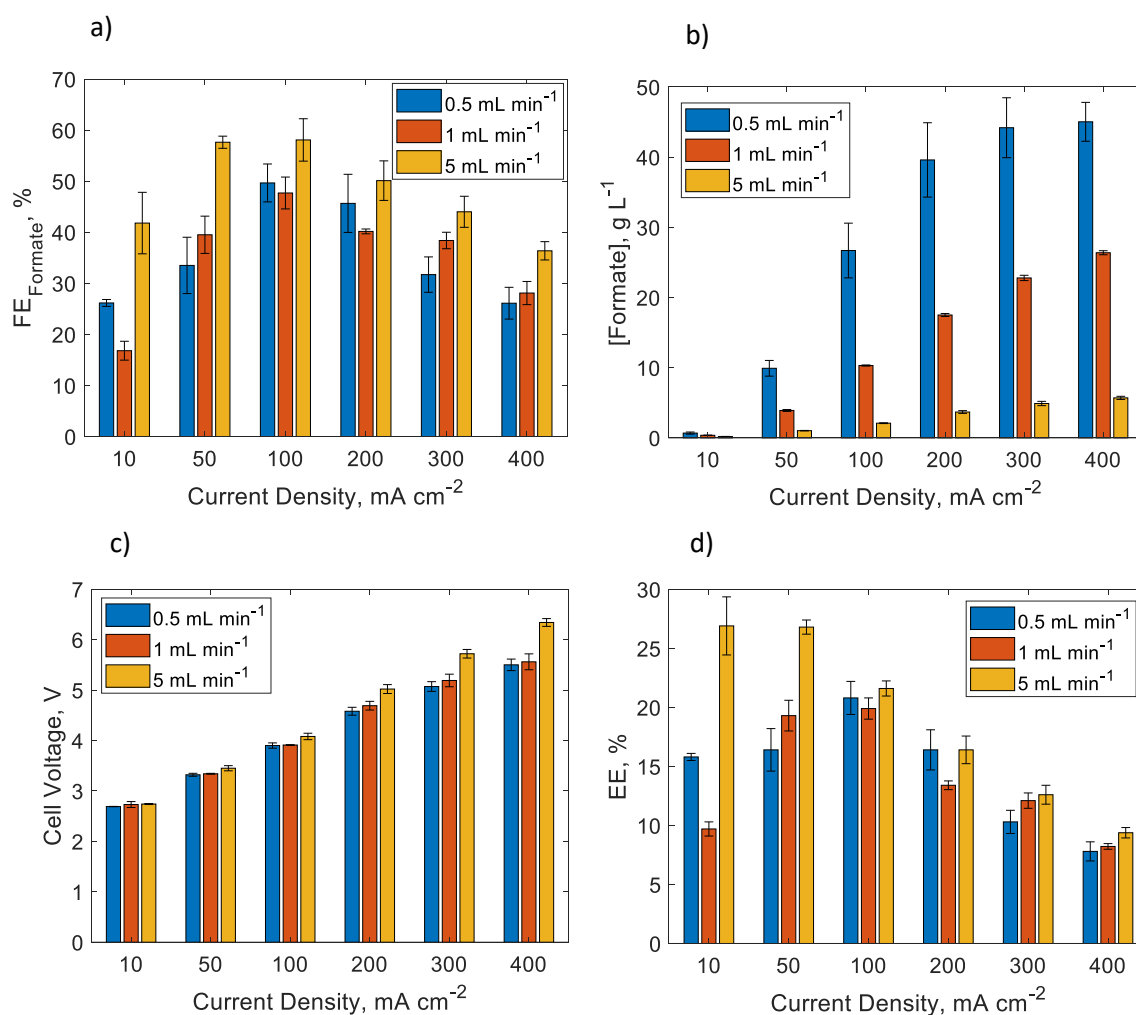
305 bicarbonate reduction, and complements the studies done so far, as mentioned previously.  
306 Therefore, SnO<sub>2</sub> coated electrodes without binder were used during the experiment as it was  
307 shown that this is the optimal composition for the conversion of bicarbonate to formate.

### 308 *3.2 Effect of the inlet flow rate*

309 While research has shown that catalyst material and electrode composition are crucial in the  
310 optimization of reactor performance, it is also important to investigate the influence of process  
311 parameters, which is currently lacking in the literature. In the first set of experiments the  
312 bicarbonate flowrate is varied between 0.5 mL min<sup>-1</sup>, 1 mL min<sup>-1</sup> and 5 mL min<sup>-1</sup> while the CD  
313 is increased from 10 mA cm<sup>-2</sup> to 400 mA cm<sup>-2</sup>. The performance of the reactor (in terms of FE)  
314 is plotted versus the applied current density in Figure 4a for the different flow rates. The overall  
315 behaviour of the evolution of FE represented with the different flow rates is very similar. At  
316 low current densities, when overpotential is low, the FE towards formate (FE<sub>Formate</sub>) is between  
317 41 and 18 % depending on the flow rate. These results are very similar to literature, where this  
318 behaviour is ascribed to the more preferred CO formation (one of the co-products often found  
319 when using Sn catalyst) at low overpotentials leading to a decrease of FE towards other carbon  
320 products such as formate, which is what we propose as an explanation of this observation.<sup>48,49</sup>  
321 However, gas phase analysis, which was not performed in this study, is needed to confirm this  
322 effect and give an exact value of FE towards CO and H<sub>2</sub>, as well as the possible energy losses  
323 present during the electrolysis. When the CD is increased towards 50 and 100 mA cm<sup>-2</sup> a sharp  
324 increase in FE<sub>Formate</sub> can be noted. A maximum FE<sub>Formate</sub> of 58 % was achieved at 5 mL min<sup>-1</sup> and  
325 100 mA cm<sup>-2</sup>. A further increase of the CD led to a linear decrease of the FE<sub>Formate</sub>, again this is  
326 similar to literature where the co-reaction HER starts dominating at increased overpotentials.<sup>23</sup>  
327 When evaluating the effect of the flow rate in eCO<sub>2</sub>R, one of the most interesting parameters  
328 to study is the concentration of formate at the outlet of the catholyte. A lower flow rate  
329 increases the retention time of the catholyte in the electrolyzer so the final concentration of  
330 formate at the outlet flow will be higher. The cost of the downstream processing to separate  
331 the formate from the rest of the solution and valorise it depends directly on its concentration.  
332 A higher concentration of formate decreases the operational costs of the downstream process.  
333 Former studies on the processing of products for conventional gas-fed CO<sub>2</sub> electrolyzers stated  
334 that, to be technologically feasible, the concentration of formate must be at least 45 g L<sup>-1</sup>.<sup>50</sup>

335 Although this concentration is calculated based on the processing of gas-fed CO<sub>2</sub> electrolyzers,  
336 it can serve as a reference for bicarbonate electrolyzers, too. In figure 4b, the concentration of  
337 formate at the outlet catholyte for each case scenario is displayed. As observed, the  
338 concentration increases significantly when the flow rate decreases, as expected. For instance,  
339 at 100 mA cm<sup>-2</sup>, it increased from 2.1 to 10 and 27 g L<sup>-1</sup> when the flow rate was 5, 1 and 0.5 mL  
340 min<sup>-1</sup>, respectively. The increase in the concentration of formate is directly proportional to the  
341 flow rate although there are small variations due to the differences in the FE for each flow rate.  
342 This trend was not strictly followed along with the screening of CD when the flow rate is 0.5  
343 mL min<sup>-1</sup> because the decrease in the FE as the CD increases is more significant (very little  
344 changes in concentration of formate from 200 to 400 mA cm<sup>-2</sup>). Interestingly when the flow  
345 rate was 0.5 mL min<sup>-1</sup>, at 200, 300 and 400 mA cm<sup>-2</sup> the concentration of formate was 40, 44  
346 and 46 g L<sup>-1</sup> respectively, very close to the target concentration for downstream processing  
347 needed for upscaling the technology, mentioned before.

348 Initially, the flow rate had no noticeable influence on the V<sub>Cell</sub> since it has the same value of 2.7  
349 V at 10 mA cm<sup>-2</sup>. Interestingly the V<sub>Cell</sub> at 5 mL min<sup>-1</sup> rose more rapidly with the CD than the  
350 experiment at 0.5 and 1 mL min<sup>-1</sup>. At 400 mA cm<sup>-2</sup>, a difference in V<sub>Cell</sub> of 800 mV was noted  
351 (figure 4c). Although with the experiments performed in this study we cannot give a precise  
352 explanation on this effect, we strongly believe the increase in the V<sub>Cell</sub> at high CD and high flow  
353 rate is caused by the loss of the stability of the electrode/electrolyte interface. More detailed  
354 research involving techniques such as Electrochemical Impedance Spectroscopy would give  
355 further information and a proper evaluation of this effect. Therefore, for the flow rates studied,  
356 since the changes in the V<sub>Cell</sub> were not significant, the variation in the EE is mostly given by the  
357 FE, following the same trend. Then, as the CD increases, the effect of the increase of the V<sub>Cell</sub>  
358 becomes noticeable and the EE decreased. The most energy-efficient systems were found at 5  
359 mL min<sup>-1</sup> and 10 and 50 mA cm<sup>-2</sup> (27 %).



360

361 **Figure 4: FE<sub>Formate</sub> (a), concentration of formate (b), V<sub>cell</sub> (c) and EE (d) of the electrolysis of a**  
 362 **KHCO<sub>3</sub> 3 M solution with a flow rate of catholyte of 0.5, 1 or 5 mL min<sup>-1</sup>. All the experiments**  
 363 **were performed using a SnO<sub>2</sub>/C electrocatalyst and KHCO<sub>3</sub> 3 M at 25 °C.**

364 From the results described above, it is clear that the most efficient performance was obtained  
 365 at increased bicarbonate flowrate, although the difference is only noticeable at 5 mL min<sup>-1</sup>.  
 366 Little difference was found between 0.5 and 1 mL min<sup>-1</sup>. It is hypothesized that this is caused  
 367 due to the longer residence time of the in-situ generated gas bubbles at a lower flow rate such  
 368 as 0.5 and 1 mL min<sup>-1</sup> (mainly CO<sub>2</sub> and H<sub>2</sub>). These bubbles will cover part of the catalyst surface  
 369 and thereby will reduce the overall electrochemical active surface area, which obviously will  
 370 negatively affect the cell's performance. However, by increasing the flow rate of the  
 371 bicarbonate, the gas/liquid ratio of the cell will decrease (e.g. more liquid will be present in the  
 372 cell) and thus less of the catalyst surface will be shielded, resulting in higher FE<sub>Formate</sub> and EE.  
 373 In addition to CO<sub>2</sub>, most of the gas formed is H<sub>2</sub> produced during the reaction. When the flow

374 rate is low, these H<sub>2</sub> bubbles stay on the surface of the electrode or in the zero-gap interface,  
375 decreasing the performance of the reactor. A higher electrolyte flow rate will mechanically  
376 remove the H<sub>2</sub> bubbles and allow most of the surface of the electrode to be fully operational  
377 for the duration of the experiment. Additionally, an increased flow rate will increase the  
378 turbulence in the cell and thereby promote the convective mass transfer of (ionic) species  
379 towards and away from the electrochemically active surface and mass transport-related losses  
380 are reduced. Finally, the retention time of the produced formate in the cell is lower at an  
381 increased flow rate, thus the crossover flux through the membrane is smaller. However, as  
382 shown in literature the crossover through BPM is rather limited thus this effect will be  
383 minimal.<sup>51,52</sup>

### 384 *3.3 Effect of the temperature of the electrolyzer*

385 We studied the effect of the temperature by building the electrolyzer up in an oven and fixing  
386 the value of the temperature in a way that the whole reactor is in isothermal conditions. By  
387 doing this, not only the KHCO<sub>3</sub> electrolyte but also the electrodes and the rest of the  
388 components of the electrolyzer will be affected by the temperature. We expected to affect the  
389 system in different ways by changing the temperature. First, the electrochemical  
390 thermodynamic parameters, such as the electrochemical reduction and oxidation potentials  
391 ( $E_{\text{red}}$  in the cathode and  $E_{\text{ox}}$  in the anode), will be decreased with the increase of temperature,  
392 as the Nernst equation indicates, leading to a decrease in the  $V_{\text{cell}}$ . On the other hand, the  
393 solubility of CO<sub>2</sub> (already low at room temperature, 0.033 M) will decrease with the increase  
394 of temperature, as Henry's law indicates and we show in Figure S1. For instance, at 40 °C the  
395 solubility of CO<sub>2</sub> in water is 0.026 M and at 60 °C the solubility is 0.018 M, decreasing the  
396 amount of dissolved CO<sub>2</sub> in the electrolyte. In a bicarbonate solution, there is always a fraction  
397 of dissolved CO<sub>2</sub> derived from the equilibrium of bicarbonate with water, which is determined  
398 by the pH (see Bjerrum plot, Figure S2). At the working pH of 8.3, this fraction is 1.2%.  
399 Therefore, in a 3 M KHCO<sub>3</sub> solution, there is 0.036 M of dissolved CO<sub>2</sub> which is higher than the  
400 solubility of CO<sub>2</sub> in water at 25 °C, 0.033 M. Thus, in a 3 M KHCO<sub>3</sub> solution at 25 °C only 0.033  
401 M remains as dissolved CO<sub>2</sub>. As the temperature increases, not only does the solubility of CO<sub>2</sub>  
402 decrease but the solubility of KHCO<sub>3</sub> increases<sup>53</sup> stabilizing the solution to detriment of the  
403 depletion of HCO<sub>3</sub><sup>-</sup> to dissolved CO<sub>2</sub> and H<sub>2</sub>O. Since in bicarbonate electrolysis the dissolved  
404 CO<sub>2</sub> is the active substrate of the reaction instead of CO<sub>2</sub> gas, it means a decrease in the amount

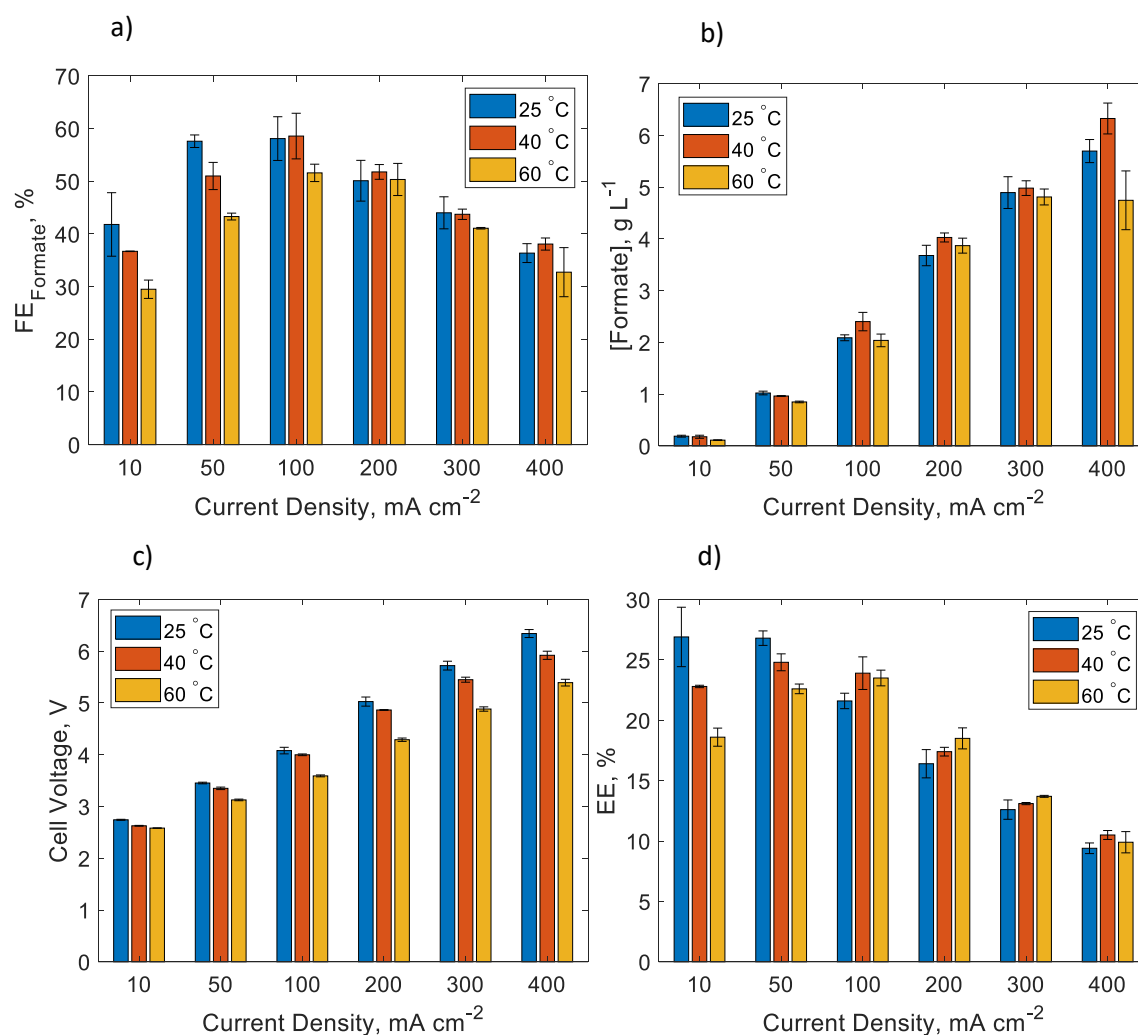


405 of available  $\text{CO}_2$  to react and thus a decrease in the FE. In addition, the thermodynamic acidic  
406 constant ( $K_{a1}$ ) of the equilibrium reaction between  $\text{HCO}_3^-$  and  $\text{CO}_2$  will be modified. The  
407 increase in temperature increases the value of the  $K_{a1}$ , meaning that the ratio  $\text{HCO}_3^-/\text{CO}_2$  will  
408 increase in favour of  $\text{HCO}_3^-$  (more  $\text{HCO}_3^-$  and less  $\text{CO}_2$  will be present at equilibrium after the  
409 BPM donates  $\text{H}^+$ ). Furthermore, the ionic conductivity of the electrolyte will increase favouring  
410 the mobility of ions, thus decreasing the resistivity of the electrolyte and improving the  $V_{\text{Cell}}$ .  
411 However, combined with the higher permeability acquired by the membrane, it might lead to  
412 product crossover, although the corresponding analysis is out of the scope of this study. We  
413 must take account the effect of the temperature on the competing reaction, HER, too. Protons  
414 are less likely to be affected by mass transport compared to  $\text{HCO}_3^-$  or  $\text{CO}_2$ , thus an increase in  
415 temperature should favor HER. Then, we can assume that increasing the temperature is  
416 favourable for decreasing the  $V_{\text{Cell}}$  but unfavourable for the electrochemical conversion of  $\text{CO}_2$   
417 (FE) since less dissolved  $\text{CO}_2$  and more  $\text{HCO}_3^-$  and  $\text{H}^+$  (HER promoters) will be available in the  
418 reactor. However, we also must take into account the effect of the temperature in the kinetics  
419 of the reaction and the diffusion of reactants. The increase of temperature promotes the  
420 exchange current density and the diffusion constant and thus the reaction rate of  $\text{CO}_2$  to  
421 formate. Nevertheless, we must investigate if the increase in the kinetics of the reaction and  
422 the decrease of the  $V_{\text{Cell}}$  is enough to overcome the drawbacks of decreasing the solubility of  
423  $\text{CO}_2$  and increasing the rate of  $\text{HCO}_3^-/\text{CO}_2$  in the electrolyte. In this regard, the EE is a parameter  
424 that can be used to evaluate the performance of each system since we can then compare both  
425 the contributions of the temperature to the  $V_{\text{Cell}}$  and the conversion of  $\text{CO}_2$  (FE).

426 To properly evaluate the effect of temperature we performed electrolysis at 25, 40 and 60 °C  
427 fixing the concentration of  $\text{KHCO}_3$  at 3 M and the flow rate at 5 mL  $\text{min}^{-1}$ . As shown in Figure  
428 5a, the  $\text{FE}_{\text{Formate}}$  decreases with the increase of temperature at CD below 100  $\text{mA cm}^{-2}$  (for  
429 instance 58, 51 and 43% at 25, 40 and 60 °C respectively) confirming the mentioned effect of  
430 the lack of dissolved  $\text{CO}_2$  present, the increase in the solubility of  $\text{KHCO}_3$  and the HER  
431 promotion at increased temperatures. After 100  $\text{mA cm}^{-2}$ , the difference of the  $\text{FE}_{\text{Formate}}$  at 25  
432 and 40 °C is not significant (44% at 300  $\text{mA cm}^{-2}$ ), but it still decreases at 60 °C (41% at 300  $\text{mA}$   
433  $\text{cm}^{-2}$ ). At 40 °C the decrease in the concentration of dissolved  $\text{CO}_2$  is compensated by the  
434 improvement in the kinetics of the reaction and the diffusion when the CD is over 100  $\text{mA cm}^{-2}$ .  
435 Below 100  $\text{mA cm}^{-2}$ , these improvements are not compensating for the lack of dissolved  $\text{CO}_2$

436 present in the electrolyte. At CD higher than  $100 \text{ mA cm}^{-2}$ , the  $\text{FE}_{\text{Formate}}$  is similar to  $25 \text{ }^\circ\text{C}$ , in  
437 contrast with  $60 \text{ }^\circ\text{C}$ , where even at high CD the low solubility of  $\text{CO}_2$  is more significant than  
438 the increase in kinetics. Another observation is that the highest  $\text{FE}_{\text{Formate}}$  obtained at  $25 \text{ }^\circ\text{C}$  is at  
439  $50 \text{ mA cm}^{-2}$  (58%), while at  $40$  and  $60 \text{ }^\circ\text{C}$  it is at  $100 \text{ mA cm}^{-2}$  (59 and 52% respectively),  
440 confirming the improvement in the kinetics of the reaction when the temperature is increased  
441 (the reaction is kinetically controlled at larger voltage). Interestingly, there is a slight shift in  
442 the trend of  $\text{FE}_{\text{Formate}}$  at increased temperature when the CD is  $>200 \text{ mA cm}^{-2}$ . This can be  
443 caused by the change in the selectivity of the reaction. As mentioned before, at higher CD, CO  
444 formation and HER are promoted, leading to a decrease in  $\text{FE}_{\text{Formate}}$ . This is an interesting effect  
445 worth of study for following bicarbonate electrolysis evaluation. In this case and contrast with  
446 the flow rate, the difference of the concentration of formate at the outlet catholyte with the  
447 temperature appears to be solely dependent on the FE, as it follows the same trend (higher  
448 FE, higher concentration). Since formic acid is not a very volatile compound at mild conditions  
449 (boiling point  $101 \text{ }^\circ\text{C}$  at 1 atm) there is not any special effect of applying  $40$  and  $60 \text{ }^\circ\text{C}$  (Figure  
450 5b).

451 If we take a look at the EE (Figure 5d), although the  $\text{FE}_{\text{Formate}}$  is lower, the system is more  
452 efficient at converting  $\text{CO}_2$  to formate at  $40$  and  $60 \text{ }^\circ\text{C}$  when the CD is higher than  $100 \text{ mA cm}^{-2}$   
453  $^2$  (13 and 14% EE at  $300 \text{ mA cm}^{-2}$  at  $40$  and  $60 \text{ }^\circ\text{C}$  respectively), due to the drastic decrease of  
454 the  $V_{\text{cell}}$  induced to the system (from  $5.7$  at  $25 \text{ }^\circ\text{C}$  to  $5.4$  and  $4.8 \text{ V}$  at  $300 \text{ mA cm}^{-2}$  at  $40$  and  $60$   
455  $^\circ\text{C}$  respectively) and the decrease of the electrolyte resistivity (Figure 5c). However, the most  
456 energy-efficient system was still at  $25 \text{ }^\circ\text{C}$ , specifically when  $50 \text{ mA cm}^{-2}$  were applied (27 %).  
457 We can then conclude that the effect of increasing the temperature is beneficial when working  
458 at a higher CD than  $100 \text{ mA cm}^{-2}$ , where the decrease in the  $V_{\text{cell}}$  has a huge impact on the EE  
459 of the system. However, CD below  $100 \text{ mA cm}^{-2}$  is still desired for achieving the highest EE. In  
460 addition, taking into account that for the EE calculations we did not consider the energy  
461 invested to heat up the system to the desired temperature (since it is a very variable parameter  
462 that depends on the setup used) we can further conclude that there is no interest in increasing  
463 the temperature if we want to achieve higher EE. This adds value to the technology as the best  
464 performance is at room temperature, a very attractive parameter for upscaling the technology.



465

466 **Figure 5: FE<sub>Formate</sub> (a), concentration of formate (b), V<sub>Cell</sub> (c) and EE (d) of the electrolysis of a**  
 467 **KHCO<sub>3</sub> solution at 25, 40 and 60 °C. All the experiments were performed using a SnO<sub>2</sub>/C**  
 468 **electrocatalyst and KHCO<sub>3</sub> 3 M at 5 mL min<sup>-1</sup>.**

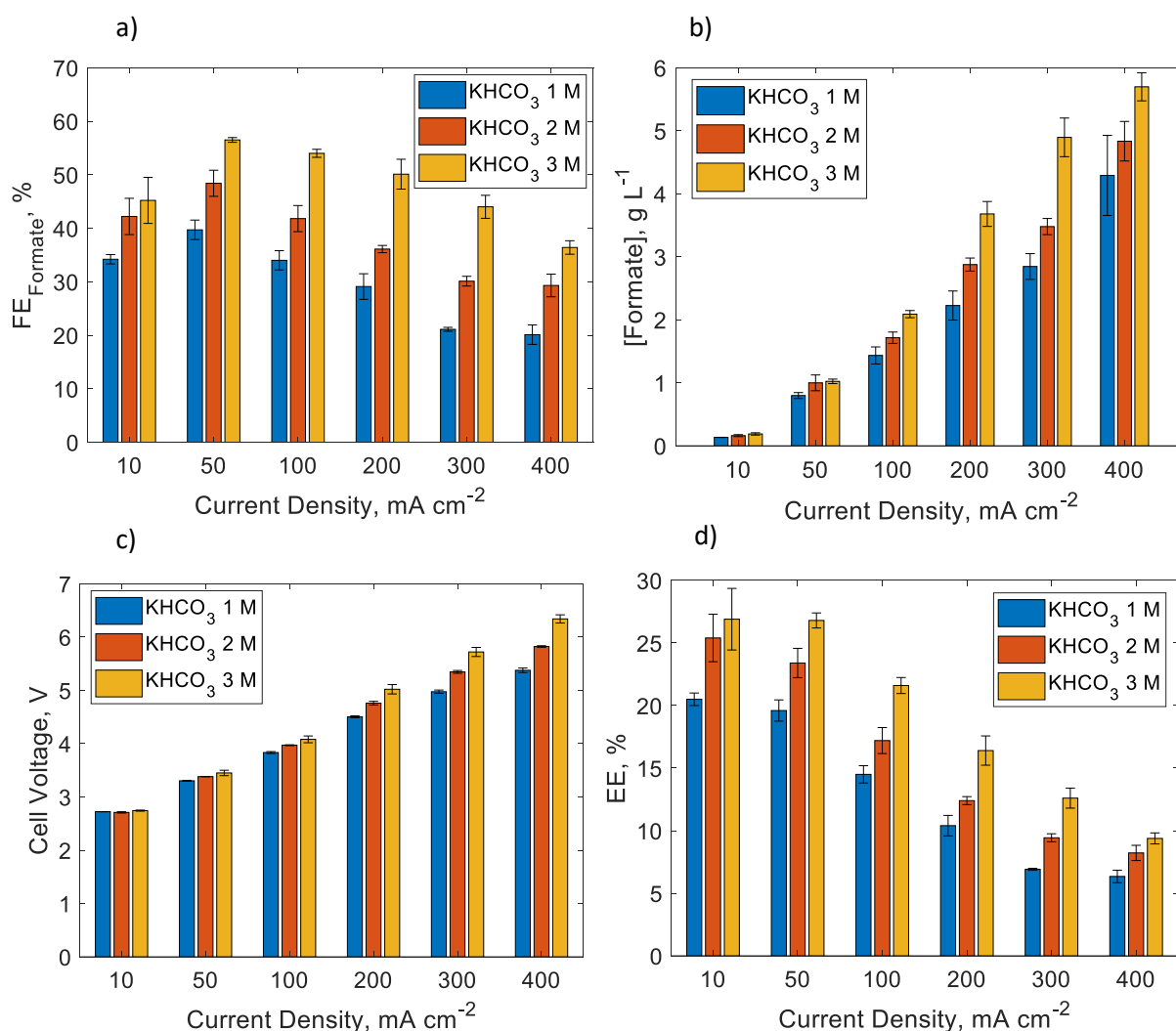
### 469 3.4 Effects of the concentration of carbon load (bicarbonate)

470 To increase the FE towards CO<sub>2</sub>R products from KHCO<sub>3</sub> electrolytes it is desired to use as high  
 471 concentration of KHCO<sub>3</sub> as possible since then the highest amount of dissolved CO<sub>2</sub> will be  
 472 present (for instance 0.036 M CO<sub>2</sub> in KHCO<sub>3</sub> 3 M, comparable to saturated CO<sub>2</sub> solutions, 0.033  
 473 M).<sup>24</sup> However, obtaining a 3 M KHCO<sub>3</sub> solution from direct air capture (DAC) or flue gas  
 474 capture using KOH solution as capturing agent is still unrealistic and ambitious from an  
 475 industrial point of view due to the low amount of CO<sub>2</sub> present in the air (415 ppm) and thus  
 476 the low concentrated KHCO<sub>3</sub> solution obtained during the capturing step. For the experiments  
 477 performed in this study up to this section, the concentration of the solution of KHCO<sub>3</sub> used as

478 electrolyte was 3 M since the highest concentration of CO<sub>2</sub> dissolved can be achieved and it  
479 was the state-of-the-art solution used in previous reports.<sup>26,31</sup> However, KHCO<sub>3</sub> 3 M is an  
480 oversaturated solution, thus unstable over time and unrealistic from a CO<sub>2</sub> capture technology  
481 perspective. Additionally, oversaturated solutions might lead to salt precipitation. For this  
482 reason, we electrolyzed unsaturated KHCO<sub>3</sub> solutions and compared them to the  
483 oversaturated KHCO<sub>3</sub> 3 M solution to evaluate if the zero-gap electrolyzer can still convert CO<sub>2</sub>  
484 from less concentrated KHCO<sub>3</sub> solutions. To perform these experiments, we fixed the  
485 temperature to 25 °C and the flow rate to 5 mL min<sup>-1</sup> and we used KHCO<sub>3</sub> solutions of 1, 2 and  
486 3 M as electrolytes. It is important to mention that, even though the initial concentration of  
487 KHCO<sub>3</sub> used as catholyte is 1, 2 or 3 M, once inside the zero-gap electrolyzer the composition  
488 of the catholyte in the electrode-membrane interface varies mainly due to the polarization of  
489 the electrode and the water depletion occurring at the BPM.<sup>28,30</sup> The main scientific reasoning  
490 says that higher concentration of bicarbonate increases the buffer strength of the catholyte,  
491 and the protons delivered from the BPM are neutralized more efficiently, releasing more CO<sub>2</sub>  
492 and decreasing HER. Nevertheless, a combination of dynamic modelling of the processes  
493 undergoing in the electrode-membrane interface with experimental data of the analysis of the  
494 inlet/outlet catholyte is needed to deliver a proper approach on the concentration of each  
495 species in the electrolyzer. However, in this section we can compare the productivity and  
496 energetic parameters of different inlet KHCO<sub>3</sub> solutions by fixing the rest of operational  
497 conditions (membrane, catalyst, flow rate and temperature).

498 The results in Figure 6a show how the FE<sub>Formate</sub> decreases when the concentration of KHCO<sub>3</sub>  
499 decreases, which was expected since less dissolved CO<sub>2</sub> and carbon donor (KHCO<sub>3</sub>) is present  
500 in the electrolyte (0.036, 0.024 and 0.012 M CO<sub>2</sub> in KHCO<sub>3</sub> 3, 2 and 1 M respectively). For  
501 instance, at 100 mA cm<sup>-2</sup>, the FE<sub>Formate</sub> goes from 58 to 41 and 33% when the concentration of  
502 KHCO<sub>3</sub> is 3, 2 and 1 M, respectively. The trend of FE<sub>Formate</sub> with the CD is the same for every  
503 KHCO<sub>3</sub> concentration used: there is an increase in the FE<sub>Formate</sub> up to 50 mA cm<sup>-2</sup> and then it  
504 decreases (slowly in KHCO<sub>3</sub> 3 M electrolytes) as the CD increases, forming a plateau from 300  
505 mA cm<sup>-2</sup> onwards when the concentration of KHCO<sub>3</sub> is 2 and 1 M. As shown, the FE<sub>Formate</sub> when  
506 using unsaturated KHCO<sub>3</sub> solutions is relatively high taking into consideration the low  
507 concentration of dissolved CO<sub>2</sub> present, although the highest FE<sub>Formate</sub> obtained is still when  
508 using oversaturated KHCO<sub>3</sub> solutions as electrolyte (as thus higher dissolved CO<sub>2</sub> present). For

509 instance, 41% of  $FE_{\text{Formate}}$  at  $50 \text{ mA cm}^{-2}$  when using  $\text{KHCO}_3$  1 M as an electrolyte is an  
 510 interesting result for upscaling technologies, taking into account that the amount of dissolved  
 511  $\text{CO}_2$  in a  $\text{KHCO}_3$  1 M solution is 0.012 M (three times less than a saturated  $\text{CO}_2$  and  $\text{KHCO}_3$   
 512 solution). This is likely caused by the proton donor ability of bicarbonate, less dominating when  
 513 the concentration is lower like 1 M. The changes in the concentration of formate at the outlet  
 514 catholyte with the different concentration of bicarbonate follow the same trend as the FE like  
 515 it happened in the case of the temperature (Figure 6b). Therefore, there is not a special role  
 516 of the initial concentration of  $\text{KHCO}_3$  on the final concentration of formate, as expected.



517

518 **Figure 6:  $FE_{\text{Formate}}$  (a), concentration of formate (b),  $V_{\text{Cell}}$  (c) and EE (d) of the electrolysis of**  
 519  **$\text{KHCO}_3$  solutions of 1, 2 and 3 M. All the experiments were performed using a  $\text{SnO}_2/\text{C}$**   
 520 **electrocatalyst and at  $5 \text{ mL min}^{-1}$  and  $25 \text{ }^\circ\text{C}$ .**

521 The  $V_{\text{Cell}}$  also decreased when the concentration of  $\text{KHCO}_3$  decreased (Figure 6c). This effect is  
522 better observed at high CD, as we previously explained when discussing the effects of the  
523 flowrate (vide supra). However, in this case, there is another parameter to consider. As  
524 observed, the  $V_{\text{Cell}}$  is not directly linked to the  $\text{FE}_{\text{Formate}}$  like it did when the flow rate was  
525 studied. For instance, from  $50 \text{ mA cm}^{-2}$  onwards, the difference in the  $\text{FE}_{\text{Formate}}$  between the  
526 three concentrations of  $\text{KHCO}_3$  used remained similar (approximately 15% between 3 and 2 M  
527 and 8% between 2 and 1 M) but the difference in the  $V_{\text{Cell}}$  increases with the CD. This is because  
528  $\text{KHCO}_3$  loses buffering effect as the concentration decreases, meaning that the acidification of  
529 the catholyte by the depletion of  $\text{H}_2\text{O}$  in the BPM will decrease the local pH close to the surface  
530 of the electrode and thus increase the concentration of  $\text{H}^+$ , decreasing the overall  $V_{\text{Cell}}$ . Even  
531 though the  $V_{\text{Cell}}$  decreases when the concentration of  $\text{KHCO}_3$  decreases (for instance 4.9, 5.3  
532 and 5.9 V at  $300 \text{ mA cm}^{-2}$  for  $\text{KHCO}_3$  1, 2 and 3 M respectively) and then we should expect an  
533 increase in the EE of the process, the EE of the conversion of  $\text{CO}_2$  is still higher as the  
534 concentration of  $\text{KHCO}_3$  is higher (Figure 6d). For instance, 15, 17 and 22% at  $100 \text{ mA cm}^{-2}$  for  
535  $\text{KHCO}_3$  1, 2 and 3 M, respectively. Therefore, in this case, the increase in the  $\text{FE}_{\text{Formate}}$  has a  
536 higher impact on the overall EE than the increase in  $V_{\text{Cell}}$ . The most energy-efficient experiment,  
537 27 %, was when using  $\text{KHCO}_3$  3 M at  $50 \text{ mA cm}^{-2}$  since the  $\text{FE}_{\text{Formate}}$  obtained is the highest  
538 (58%) and the polarization of the electrode is not enough to increase the  $V_{\text{Cell}}$  significantly (3.3,  
539 3.4 and 3.5 V for  $\text{KHCO}_3$  1, 2 and 3 M respectively). As an additional observation, salt  
540 precipitation (a common drawback when using high concentrations of bicarbonate) was not  
541 observed in any of the experiments performed, even when using oversaturated solutions (3  
542 M). We attribute it to the acidification effect of BPM which converts bicarbonate to  $\text{CO}_2$  in-situ  
543 the electrolysis and controls the pH gradients during the reaction, giving extra value to the  
544 technology.

#### 545 **4 Conclusions**

546 Due to the necessity to reduce the costs of the overall  $\text{CO}_2$  Capture and Conversion systems,  
547 the attention is focused not only on the optimization of the  $\text{CO}_2$  electrochemical reactors but  
548 also on the capture and release of  $\text{CO}_2$  to the electrochemical cell. Bicarbonate reduction,  
549 which was declared inefficient and its applicability was in doubt, is starting to gain attention  
550 since it is one of the most promising routes towards developing an efficient integrated  $\text{CO}_2$   
551 capture and conversion system involving the electrochemical reduction of  $\text{CO}_2$ . Thanks to the

552 recent knowledge gained in reactor design and on the mechanism of bicarbonate reduction,  
553 the process is now feasible at a lab scale and easier to be upscaled. In this manuscript, we have  
554 displayed how different engineering aspects such as the inlet flow rate, the temperature of the  
555 reactor or the concentration of bicarbonate, not yet evaluated for the current reactor used for  
556 bicarbonate conversion (zero-gap electrolyzer involving a BPM as a separator) affect the  
557 parameters often used to evaluate the performance of an eCO<sub>2</sub>R electrolyzer such as the CD,  
558 the FE, the concentration of product formed, the  $V_{\text{cell}}$  and the EE. Overall, the most efficient  
559 systems were found at low CD (10, 50 mA cm<sup>-2</sup>), high flow rate (5 mL min<sup>-1</sup>), room temperature  
560 and high KHCO<sub>3</sub> concentration (3 M), with a maximum EE of 27% (well comparable to  
561 commonly reported EE in gas-fed CO<sub>2</sub> electrolyzers). Nevertheless, from a product processing  
562 perspective, the most interesting system is found at a low flow rate (> 40 g L<sup>-1</sup> of formate were  
563 produced at 0.5 mL min<sup>-1</sup>). However, there is still room to improve the performance of the  
564 bicarbonate electrolyzer. It is observed that the best performance was obtained at 5 mL min<sup>-1</sup>,  
565 then it is interesting to evaluate in further research the effect of higher flow rate, for instance  
566 at 50 mL min<sup>-1</sup>. On the other hand, one of the biggest reasons for the loss of EE of the system  
567 is the increase of  $V_{\text{cell}}$  with the applied CD due to the use of BPM. Therefore, new and more  
568 optimized BPM can be used to minimize the Ohmic drop which requires to be alert on the  
569 research done on BPM technology, since it is a relatively new field of application for eCO<sub>2</sub>R  
570 (few commercial BPM are currently available). Additionally, the decrease of Ohmic drop would  
571 enable testing higher CDs (> 400 mA cm<sup>-2</sup>) at lower  $V_{\text{cell}}$ . Other options for membranes have  
572 been considered, however, the ability of BPM to maintain the pH gradients and product  
573 crossover (in addition to the additional application of generating protons to produce CO<sub>2</sub> from  
574 bicarbonate) makes the BPM the best choice for upscaling bicarbonate electrolyzers.<sup>54</sup> Further  
575 understanding of the effects of different parameters, such as the ones considered in our study,  
576 on the ohmic and the charge transfer resistance of the reactor is still needed. For example,  
577 elaborating a deep study including techniques such as Electrochemical Impedance  
578 Spectroscopy will allow us to understand better how the flow rate and the retention of bubbles  
579 affect the performance of the bicarbonate zero-gap electrolyzer. Another urgent approach we  
580 are currently following is to target other carbon products which high valorization, such as  
581 methanol or C<sub>2</sub> products, by testing Cu-based electrocatalyst, still unreported. Finally, the  
582 electrocatalyst can be further optimized, especially focusing on its stability. The system's EE  
583 drops to 27 to 17% after 3 hours of reaction time (Figure S3) which is assumed because of the

584 loss of catalyst activity, probably caused by the lack of binder material during the electrode  
585 manufacturing (Figure S4).<sup>55,56</sup> Nonetheless the findings in this work show promising results  
586 towards the implementation of fine-designed bicarbonate electrolyzers for the integrated  
587 capture and conversion of CO<sub>2</sub>.

## 588 **Supporting Information**

589 Formulas and equations, Bjerrum plot, Henry's law's model, stability test, etc.

## 590 **Conflicts of interest**

591 There are no conflicts to declare.

## 592 **Acknowledgements**

593 O.G.S. is supported by a PhD grant from VITO's strategic research funds (project no. 1810257).  
594 B.D.M is supported by the University of Antwerp's Strategic Basic Research Industrial  
595 Research Fund (BSO-IOF) (project no. FF1170350). This research was also supported by the  
596 project CAPTIN (under the Moonshot initiative of VLAIO/Catalisti, Grant number  
597 HBC.2019.0076).

## 598 **References**

- 599 (1) Aresta, M. Carbon Dioxide: Utilization Options to Reduce Its Accumulation in the  
600 Atmosphere. In *Carbon Dioxide as Chemical Feedstock*; Wiley-VCH Verlag GmbH & Co.  
601 KGaA: Weinheim, Germany; pp 1–13.
- 602 (2) Nagelkerken, I.; Connell, S. D. Global Alteration of Ocean Ecosystem Functioning Due  
603 to Increasing Human CO<sub>2</sub> Emissions. *Proceedings of the National Academy of Sciences*  
604 **2015**, *112* (43), 13272–13277.
- 605 (3) Dietz, T.; Rosa, E. A. Effects of Population and Affluence on CO<sub>2</sub> Emissions. *Proceedings*  
606 *of the National Academy of Sciences* **1997**, *94* (1), 175–179.
- 607 (4) Grim, R. G.; Huang, Z.; Guarnieri, M. T.; Ferrell, J. R.; Tao, L.; Schaidle, J. A. Transforming  
608 the Carbon Economy: Challenges and Opportunities in the Convergence of Low-Cost  
609 Electricity and Reductive CO<sub>2</sub> Utilization. *Energy & Environmental Science* **2020**, *13* (2),  
610 472–494.



- 611 (5) Sullivan, I.; Goryachev, A.; Digdaya, I. A.; Li, X.; Atwater, H. A.; Vermaas, D. A.; Xiang, C.  
612 Coupling Electrochemical CO<sub>2</sub> Conversion with CO<sub>2</sub> Capture. *Nature Catalysis* **2021**, *4*  
613 (11), 952–958.
- 614 (6) Sánchez, O. G.; Birdja, Y. Y.; Bulut, M.; Vaes, J.; Breugelmans, T.; Pant, D. Recent  
615 Advances in Industrial CO<sub>2</sub> Electroreduction. *Current Opinion in Green and Sustainable*  
616 *Chemistry* **2019**, *16*, 47–56.
- 617 (7) Choukroun, D.; Pacquets, L.; Li, C.; Hoekx, S.; Arnouts, S.; Baert, K.; Hauffman, T.; Bals,  
618 S.; Breugelmans, T. Mapping Composition–Selectivity Relationships of Supported Sub-  
619 10 Nm Cu–Ag Nanocrystals for High-Rate CO<sub>2</sub> Electroreduction. *ACS Nano* **2021**,  
620 acsnano.1c04943.
- 621 (8) Karapinar, D.; Creissen, C. E.; Rivera de la Cruz, J. G.; Schreiber, M. W.; Fontecave, M.  
622 Electrochemical CO<sub>2</sub> Reduction to Ethanol with Copper-Based Catalysts. *ACS Energy*  
623 *Letters* **2021**, *6* (2), 694–706.
- 624 (9) Artz, J.; Müller, T. E.; Thenert, K.; Kleinekorte, J.; Meys, R.; Sternberg, A.; Bardow, A.;  
625 Leitner, W. Sustainable Conversion of Carbon Dioxide: An Integrated Review of  
626 Catalysis and Life Cycle Assessment. *Chemical Reviews* **2018**, *118* (2), 434–504.
- 627 (10) Zhao, S.; Li, S.; Guo, T.; Zhang, S.; Wang, J.; Wu, Y.; Chen, Y. Advances in Sn-Based  
628 Catalysts for Electrochemical CO<sub>2</sub> Reduction. *Nano-Micro Letters* **2019**, *11* (1), 62.
- 629 (11) Brandl, P.; Bui, M.; Hallett, J. P.; Mac Dowell, N. Beyond 90% Capture: Possible, but at  
630 What Cost? *International Journal of Greenhouse Gas Control* **2021**, *105*, 103239.
- 631 (12) Oh, S.-Y.; Binns, M.; Cho, H.; Kim, J.-K. Energy Minimization of MEA-Based CO<sub>2</sub> Capture  
632 Process. *Applied Energy* **2016**, *169*, 353–362.
- 633 (13) Rinberg, A.; Bergman, A. M.; Schrag, D. P.; Aziz, M. J. Alkalinity Concentration Swing for  
634 Direct Air Capture of Carbon Dioxide. *ChemSusChem* **2021**, cssc.202100786.
- 635 (14) Keith, D. W.; Holmes, G.; St. Angelo, D.; Heidel, K. A Process for Capturing CO<sub>2</sub> from the  
636 Atmosphere. *Joule* **2018**, *2* (8), 1573–1594.
- 637 (15) Gutiérrez-Sánchez, O.; Bohlen, B.; Daems, N.; Bulut, M.; Pant, D.; Breugelmans, T. A  
638 State-of-the-Art Update on Integrated CO<sub>2</sub> Capture and Electrochemical Conversion  
639 Systems. *ChemElectroChem* **2022**.
- 640 (16) Welch, A. J.; Dunn, E.; DuChene, J. S.; Atwater, H. A. Bicarbonate or Carbonate  
641 Processes for Coupling Carbon Dioxide Capture and Electrochemical Conversion. *ACS*  
642 *Energy Letters* **2020**, *5* (3), 940–945.

- 643 (17) Wakerley, D.; Lamaison, S.; Wicks, J.; Clemens, A.; Feaster, J.; Corral, D.; Jaffer, S. A.;  
644 Sarkar, A.; Fontecave, M.; Duoss, E. B.; Baker, S.; Sargent, E. H.; Jaramillo, T. F.; Hahn,  
645 C. Gas Diffusion Electrodes, Reactor Designs and Key Metrics of Low-Temperature CO<sub>2</sub>  
646 Electrolysers. *Nature Energy* **2022**, 7 (2), 130–143.
- 647 (18) Bonet Navarro, A.; Nogalska, A.; Garcia-Valls, R. Direct Electrochemical Reduction of  
648 Bicarbonate to Formate Using Tin Catalyst. *Electrochem* **2021**, 2 (1), 64–70.
- 649 (19) Sreekanth, N.; Phani, K. L. Selective Reduction of CO<sub>2</sub> to Formate through Bicarbonate  
650 Reduction on Metal Electrodes: New Insights Gained from SG/TC Mode of SECM. *Chem.*  
651 *Commun.* **2014**, 50 (76), 11143–11146.
- 652 (20) Goyal, A.; Marcandalli, G.; Mints, V. A.; Koper, M. T. M. Competition between CO<sub>2</sub>  
653 Reduction and Hydrogen Evolution on a Gold Electrode under Well-Defined Mass  
654 Transport Conditions. *J Am Chem Soc* **2020**, 142 (9), 4154–4161.
- 655 (21) Deng, W.; Yuan, T.; Chen, S.; Li, H.; Hu, C.; Dong, H.; Wu, B.; Wang, T.; Li, J.; Ozin, G. A.;  
656 Gong, J. Effect of Bicarbonate on CO<sub>2</sub> Electroreduction over Cathode Catalysts.  
657 *Fundamental Research* **2021**, 1 (4), 432–438.
- 658 (22) Dunwell, M.; Lu, Q.; Heyes, J. M.; Rosen, J.; Chen, J. G.; Yan, Y.; Jiao, F.; Xu, B. The Central  
659 Role of Bicarbonate in the Electrochemical Reduction of Carbon Dioxide on Gold. *J Am*  
660 *Chem Soc* **2017**, 139 (10), 3774–3783.
- 661 (23) Ooka, H.; Figueiredo, M. C.; Koper, M. T. M. Competition between Hydrogen Evolution  
662 and Carbon Dioxide Reduction on Copper Electrodes in Mildly Acidic Media. *Langmuir*  
663 **2017**, 33 (37), 9307–9313.
- 664 (24) Gutiérrez-Sánchez, O.; Daems, N.; Offermans, W.; Birdja, Y. Y.; Bulut, M.; Pant, D.;  
665 Breugelmans, T. The Inhibition of the Proton Donor Ability of Bicarbonate Promotes  
666 the Electrochemical Conversion of CO<sub>2</sub> in Bicarbonate Solutions. *Journal of CO<sub>2</sub>*  
667 *Utilization* **2021**, 48, 101521.
- 668 (25) Gutierrez-Sanchez, O.; Daems, N.; Bulut, M.; Deepak, P.; Breugelmans, T. Effects of  
669 Benzyl Functionalized Cationic Surfactants on the Inhibition of the Hydrogen Evolution  
670 Reaction in CO<sub>2</sub> Reduction Systems. *ACS Applied Materials & Interfaces* **2021**, 13, 47,  
671 56205–56216.
- 672 (26) Li, T.; Lees, E. W.; Zhang, Z.; Berlinguette, C. P. Conversion of Bicarbonate to Formate  
673 in an Electrochemical Flow Reactor. *ACS Energy Letters* **2020**, 5 (8), 2624–2630.

- 674 (27) Li, T.; Lees, E. W.; Goldman, M.; Salvatore, D. A.; Weekes, D. M.; Berlinguette, C. P.  
675 Electrolytic Conversion of Bicarbonate into CO in a Flow Cell. *Joule* **2019**, 3 (6), 1487–  
676 1497.
- 677 (28) de Mot, B.; Hereijgers, J.; Daems, N.; Breugelmans, T. Insight in the Behavior of Bipolar  
678 Membrane Equipped Carbon Dioxide Electrolyzers at Low Electrolyte Flowrates.  
679 *Chemical Engineering Journal* **2022**, 428, 131170.
- 680 (29) Vermaas, D. A.; Smith, W. A. Synergistic Electrochemical CO<sub>2</sub> Reduction and Water  
681 Oxidation with a Bipolar Membrane. *ACS Energy Letters* **2016**, 1 (6), 1143–1148.
- 682 (30) Ramdin, M.; Morrison, A. R. T.; de Groen, M.; van Haperen, R.; de Kler, R.; van den  
683 Broeke, L. J. P.; Trusler, J. P. M.; de Jong, W.; Vlugt, T. J. H. High Pressure  
684 Electrochemical Reduction of CO<sub>2</sub> to Formic Acid/Formate: A Comparison between  
685 Bipolar Membranes and Cation Exchange Membranes. *Industrial & Engineering*  
686 *Chemistry Research* **2019**, 58 (5), 1834–1847.
- 687 (31) Lees, E. W.; Goldman, M.; Fink, A. G.; Dvorak, D. J.; Salvatore, D. A.; Zhang, Z.; Loo, N.  
688 W. X.; Berlinguette, C. P. Electrodes Designed for Converting Bicarbonate into CO. *ACS*  
689 *Energy Letters* **2020**, 2165–2173.
- 690 (32) Jouny, M.; Luc, W.; Jiao, F. General Techno-Economic Analysis of CO<sub>2</sub> Electrolysis  
691 Systems. *Industrial & Engineering Chemistry Research* **2018**, 57 (6), 2165–2177.
- 692 (33) Ramdin, M.; Morrison, A. R. T.; de Groen, M.; van Haperen, R.; de Kler, R.; Irtem, E.;  
693 Laitinen, A. T.; van den Broeke, L. J. P.; Breugelmans, T.; Trusler, J. P. M.; Jong, W. de;  
694 Vlugt, T. J. H. High-Pressure Electrochemical Reduction of CO<sub>2</sub> to Formic Acid/Formate:  
695 Effect of PH on the Downstream Separation Process and Economics. *Industrial &*  
696 *Engineering Chemistry Research* **2019**, 58 (51), 22718–22740.
- 697 (34) Jiang, J.; Wieckowski, A. Prospective Direct Formate Fuel Cell. *Electrochemistry*  
698 *Communications* **2012**, 18, 41–43.
- 699 (35) An, L.; Chen, R. Direct Formate Fuel Cells: A Review. *Journal of Power Sources* **2016**,  
700 320, 127–139.
- 701 (36) Kortlever, R.; Tan, K. H.; Kwon, Y.; Koper, M. T. M. Electrochemical Carbon Dioxide and  
702 Bicarbonate Reduction on Copper in Weakly Alkaline Media. *Journal of Solid State*  
703 *Electrochemistry* **2013**, 17 (7), 1843–1849.
- 704 (37) Li, T.; Lees, E. W.; Zhang, Z.; Berlinguette, C. P. Conversion of Bicarbonate to Formate  
705 in an Electrochemical Flow Reactor. *ACS Energy Letters* **2020**, 5 (8), 2624–2630.

- 706 (38) de Mot, B.; Hereijgers, J.; Duarte, M.; Breugelmans, T. Influence of Flow and Pressure  
707 Distribution inside a Gas Diffusion Electrode on the Performance of a Flow-by CO<sub>2</sub>  
708 Electrolyzer. *Chemical Engineering Journal* **2019**, *378*, 122224.
- 709 (39) Akbashev, A. R. Electrocatalysis Goes Nuts. *ACS Catalysis* **2022**, 4296–4301.
- 710 (40) del Castillo, A.; Alvarez-Guerra, M.; Solla-Gullón, J.; Sáez, A.; Montiel, V.; Irabien, A.  
711 Electrocatalytic Reduction of CO<sub>2</sub> to Formate Using Particulate Sn Electrodes: Effect of  
712 Metal Loading and Particle Size. *Applied Energy* **2015**, *157*, 165–173.
- 713 (41) de Mot, B.; Ramdin, M.; Hereijgers, J.; Vlugt, T. J. H.; Breugelmans, T. Direct Water  
714 Injection in Catholyte-Free Zero-Gap Carbon Dioxide Electrolyzers. *ChemElectroChem*  
715 **2020**, *7* (18), 3839–3843.
- 716 (42) Liu, H.; Miao, B.; Chuai, H.; Chen, X.; Zhang, S.; Ma, X. Nanoporous Tin Oxides for  
717 Efficient Electrochemical CO<sub>2</sub> Reduction to Formate. *Green Chemical Engineering*  
718 **2021**.
- 719 (43) Al-Tamreh, S. A.; Ibrahim, M. H.; El-Naas, M. H.; Vaes, J.; Pant, D.; Benamor, A.;  
720 Amhamed, A. Electroreduction of Carbon Dioxide into Formate: A Comprehensive  
721 Review. *ChemElectroChem* **2021**, *8* (17), 3207–3220.
- 722 (44) Damas, G. B.; Miranda, C. R.; Sgarbi, R.; Portela, J. M.; Camilo, M. R.; Lima, F. H. B.;  
723 Araujo, C. M. On the Mechanism of Carbon Dioxide Reduction on Sn-Based Electrodes:  
724 Insights into the Role of Oxide Surfaces. *Catalysts* **2019**, *9* (8), 636.
- 725 (45) Baruch, M. F.; Pander, J. E.; White, J. L.; Bocarsly, A. B. Mechanistic Insights into the  
726 Reduction of CO<sub>2</sub> on Tin Electrodes Using in Situ ATR-IR Spectroscopy. *ACS Catalysis*  
727 **2015**, *5* (5), 3148–3156.
- 728 (46) Merino-Garcia, I.; Tinat, L.; Albo, J.; Alvarez-Guerra, M.; Irabien, A.; Durupthy, O.; Vivier,  
729 V.; Sánchez-Sánchez, C. M. Continuous Electroconversion of CO<sub>2</sub> into Formate Using 2  
730 Nm Tin Oxide Nanoparticles. *Applied Catalysis B: Environmental* **2021**, *297*, 120447.
- 731 (47) Kutz, R. B.; Chen, Q.; Yang, H.; Sajjad, S. D.; Liu, Z.; Masel, I. R. Sustainion Imidazolium-  
732 Functionalized Polymers for Carbon Dioxide Electrolysis. *Energy Technology* **2017**, *5* (6),  
733 929–936.
- 734 (48) Li, C. W.; Kanan, M. W. CO<sub>2</sub> Reduction at Low Overpotential on Cu Electrodes Resulting  
735 from the Reduction of Thick Cu<sub>2</sub>O Films. *J Am Chem Soc* **2012**, *134* (17), 7231–7234.
- 736 (49) Feaster, J. T.; Shi, C.; Cave, E. R.; Hatsukade, T.; Abram, D. N.; Kuhl, K. P.; Hahn, C.;  
737 Nørskov, J. K.; Jaramillo, T. F. Understanding Selectivity for the Electrochemical

738 Reduction of Carbon Dioxide to Formic Acid and Carbon Monoxide on Metal  
739 Electrodes. *ACS Catalysis* **2017**, 7 (7), 4822–4827.

740 (50) Oloman, C.; Li, H. Electrochemical Processing of Carbon Dioxide. *ChemSusChem* **2008**,  
741 1 (5), 385–391.

742 (51) Li, Y. C.; Yan, Z.; Hitt, J.; Wycisk, R.; Pintauro, P. N.; Mallouk, T. E. Bipolar Membranes  
743 Inhibit Product Crossover in CO<sub>2</sub> Electrolysis Cells. *Advanced Sustainable Systems* **2018**,  
744 1700187, 1700187.

745 (52) Wang, N.; Miao, R. K.; Lee, G.; Vomiero, A.; Sinton, D.; Ip, A. H.; Liang, H.; Sargent, E. H.  
746 Suppressing the Liquid Product Crossover in Electrochemical CO<sub>2</sub> Reduction. *SmartMat*  
747 **2021**, 2 (1), 12–16.

748 (53) Bourcier, W. L.; Stolaroff, J. K.; Smith, M. M.; Aines, R. D. Achieving Supercritical Fluid  
749 CO<sub>2</sub> Pressures Directly from Thermal Decomposition of Solid Sodium Bicarbonate.  
750 *Energy Procedia* **2017**, 114, 2545–2551.

751 (54) Blommaert, M. A.; Aili, D.; Tufa, R. A.; Li, Q.; Smith, W. A.; Vermaas, D. A. Insights and  
752 Challenges for Applying Bipolar Membranes in Advanced Electrochemical Energy  
753 Systems. *ACS Energy Letters* **2021**, 6 (7), 2539–2548.

754 (55) Franzen, D.; Ellendorff, B.; Paulisch, M. C.; Hilger, A.; Osenberg, M.; Manke, I.; Turek, T.  
755 Influence of Binder Content in Silver-Based Gas Diffusion Electrodes on Pore System  
756 and Electrochemical Performance. *Journal of Applied Electrochemistry* **2019**, 49 (7),  
757 705–713.

758 (56) Arinton, G.; Rianto, A.; Faizal, F.; Hidayat, D.; Hidayat, S.; Panatarani, C.; Joni, I. M. Effect  
759 of Binders on Natural Graphite Powder-Based Gas Diffusion Electrode for Mg-Air Cell;  
760 2016; p 030055.

761

762

763

764

765

766

767

